JOURNAL OF GEOPHYSICAL RESEARCH, VOL. 101, NO. A8, PAGES 17,399–17,408, AUGUST 1, 1996

Structure, phase motion, and heating within Alfvén resonances

Andrew N. Wright[1] and W. Allan

National Institute of Water and Atmospheric Research, Wellington, New Zealand

Abstract. An analytical investigation of Alfvén resonances is presented for the cases when energy is dissipated by (1) resistivity (η) within the body of the plasma, and (2) finite Pedersen conductivity (Σ_p) within the ionospheric boundaries. Universal functions for both solutions are compared, and we find that the structure and phase motion of the resonant fields is fairly insensitive to the details of dissipation. We also identify a curious property of resonances: the spatially integrated (but not time-averaged) dissipation rate is independent of time for whichever dissipation process we consider. It appears that resonances have a remarkably robust structure.

1. Introduction

Resonant MHD wave coupling is important for understanding the behavior of nonuniform magnetoplasmas. In the solar corona it is thought that resonant excitation of Alfvén waves may enable us to understand the unusually high temperatures there [*Ionson*, 1978], and the same basic mechanism is also employed for heating laboratory plasmas [*Vaclavik and Appert*, 1991, and references therein]. In the Earth's magnetosphere the same coupling process is believed to establish low-frequency pulsations [*Southwood*, 1974; *Chen and Hasegawa*, 1974].

There have been many numerical and analytical investigations of resonant wave coupling [see, e.g., *Wright and Rickard*, 1995; *Goossens and Ruderman*, 1995; *Goossens et al.*, 1995, and references therein]. Hereafter *Goossens et al.* [1995] is referred to as GRH. *Wright and Rickard* [1995] identified some curious features of the resonance in a numerical study when plasma resistivity was included. They identified waves of ohmic heating that have a phase motion across the resonant layer in the direction of decreasing Alfvén frequency. Here we make a connection between this property and observations of resonances in the Earth's magnetosphere that show poleward motion of the electric field. *Wright and Rickard* [1995] also noted that their numerical results showed the spatially integrated (but not time-averaged) ohmic heating rate was independent of time. We have been able to investigate this claim further here by employing the novel anaytical solution derived by GRH. They expressed the solution for a resistive plasma in terms of "universal" functions which have an analytical form. By employing the results of GRH, we are able to find analytical expressions for the ohmic heating waves and confirm the numerical results of *Wright and Rickard* [1995].

The resistivity of magnetospheric plasma provides much less dissipation than the resistive ionosphere. In this paper we derive analogous universal functions for the case when the resonance is limited by ionospheric dissipation rather than resistivity within the body of the plasma. We find that the two sets of universal functions are qualitatively very similar, and this suggests that the structure of resonances is quite robust and insensitive to the nature of the dissipation. The solution determined by ionospheric dissipation also exhibits phase motion across the resonance and a spatially integrated ohmic heating rate that is independent of time. We have no physical explanation of the latter property, although it is evidently a fairly general property of resonances regardless of the exact details of the dissipation mechanism.

2. Governing Equations

We seek normal mode solutions to the cold linearized MHD equations in a one-dimensional box model in which the background magnetic field ($\mathbf{B}$) is uniform, and the density (ρ) is solely a function of x. The perturbations have a dependence on time (t) and y of

$$\exp i(k_y y - \omega t) \tag{1}$$

The ends of the field lines are terminated in plane boundaries at $z = \pm\ell$ which may represent the ionosphere or photosphere. The waves stand between the boundaries and vary with z according to

$$u_x, u_y, b_z \sim \cos(k_z z); \qquad b_x, b_y \sim \sin(k_z z) \tag{2}$$

for the odd modes. (The even modes have the opposite sin / cos dependence.) Since the fundamental mode

[1] On leave from Mathematical Institute, University of St. Andrews, St. Andrews, Fife, Scotland.

Paper number 96JA01141.
0148-0227/96/96JA-01141$09.00

is likely to be of most interest, we shall adopt the dependence given in (2) for the remainder of the paper. When the terminating boundaries are perfectly reflecting/conducting, the wavenumber k_z is real and is quantized by requiring that the electric field vanish there. If the boundaries are not perfect reflectors, k_z is complex and the boundaries absorb energy [*Newton et al.*, 1978; *Allan and Knox*, 1979; *Southwood and Hughes*, 1983].

We also allow for the fact that the magnetic diffusivity ($\eta = 1/(\mu_0\sigma)$, σ being the electrical conductivity) within the body of the plasma may be important. Under these conditions the governing momentum and induction equations for the Fourier coefficients $b_x(x)$, $u_x(x)$, ..., etc., may be written

$$-i\omega u_x = \frac{V^2}{B}\left(k_z b_x - \frac{db_z}{dx}\right) \quad (3a)$$

$$-i\omega u_y = \frac{V^2}{B}(k_z b_y - ik_y b_z) \quad (3b)$$

$$-i\omega b_x = -Bk_z u_x + \eta\nabla^2 b_x \quad (3c)$$

$$-i\omega b_y = -Bk_z u_y + \eta\nabla^2 b_y \quad (3d)$$

$$-i\omega b_z = -B\left(\frac{du_x}{dx} + ik_y u_y\right) + \eta\nabla^2 b_z \quad (3e)$$

where $\nabla^2 = d^2/dx^2 - k_y^2 - k_z^2$ and V is the local Alfvén speed ($V^2 = B^2/\mu_0\rho(x)$). Note we are assuming that plasma pressure remains negligible compared to magnetic pressure, despite the fact that the plasma may suffer ohmic heating. This is acceptable so long as the heat is radiated or conducted away on a shorter timescale than the period of the waves.

3. Resistive Plasma Solutions

In section 3 we consider the case of perfectly reflecting boundaries in z (i.e., k_z is real) but allow η to be nonzero. This problem has been studied in an elegant paper by *Goossens et al.* [1995] (GRH), and references therein. Such a model is thought to be applicable to resonant wave coupling in solar coronal flux tubes. Although GRH were working in a cylindrical geometry, we present their results below in the Cartesian "box model" by taking an appropriate limit of their solution.

GRH note that the resonance has a finite width due to the resistivity of the plasma of order δ_A,

$$\delta_A = \left(\frac{\omega\eta}{\Delta}\right)^{1/3} \quad (4)$$

where $\Delta = -d\omega_A^2/dx$ and ω_A is the natural Alfvén frequency of the field line ($\omega_A^2 = k_z^2V^2$). Thus it is convenient to adopt a scaled variable (τ) to describe the structure across the resonant layer.

$$\tau = \frac{x - x_r}{\delta_A} \quad (5)$$

where x_r is the position of the Alfvén resonance: $\omega_A^2(x_r) = \omega^2$. Note that we have omitted the modulus sign in (4) compared with GRH's equation (53). The result is that our δ_A may be positive or negative, and so τ increases in the direction of decreasing ω_A^2, rather than GRH's τ which always increases with increasing x. (This redefinition allows us to drop all the modulus and *sign* terms from the analysis of GRH.)

GRH show that the x or τ dependence of the waves can be described in terms of universal functions F and G which have the following integral definitions.

$$F(\tau) = \int_0^\infty \exp(iu\tau - u^3/3)du \quad (6a)$$

$$G(\tau) = \int_0^\infty \frac{e^{-u^3/3}}{u}(\exp(iu\tau) - 1)du \quad (6b)$$

Close to the resonance the wave solution is characterized by the following variations with x, which we express in terms of τ,

$$\xi_x \propto G(\tau) + const \quad (7a)$$

$$\xi_y \propto F(\tau) \quad (7b)$$

$$b_z \propto const \quad (7c)$$

where the plasma displacement ($\boldsymbol{\xi}$) and velocity are related by $\mathbf{u} = -i\omega\boldsymbol{\xi}$. The functions F and G have also been found to govern the structure of the resonant layer when it is limited by viscosity [*Hollweg and Yang*, 1988] and are displayed here in Figures 1 and 2.

The structure of the resistive resonance has been investigated numerically recently by *Wright and Rickard* [1995], who noted that waves of ohmic heating (equal to $\mu_0\eta j_z^2$ in the small η limit) propagated through the resistive layer (see their Figure 12). They also noted a surprising feature of the heating; namely, that when integrated over space, it was independent of time. *Wright and Rickard* [1995] arrived at these results by solving the time-dependent resistive governing equations with a steady harmonic driver, $\exp(i\omega t)$, and running their simulation long enough for transients to decay away.

The results of GRH in (6) and (7) permit the possibility of examining the numerically derived conclusions of *Wright and Rickard* [1995] from an analytical standpoint. We begin with the expression for ξ_y,

$$\xi_y = \frac{Ae^{i\phi}}{\delta_A\Delta} \cdot F(\tau) \quad (8)$$

where A is a real constant dependent upon equilibrium quantities and the amplitude of the wave and ϕ is the arbitrary phase of the solution. Next we find b_y from (3d) noting that the second term on the right is of the order of $\eta^{1/3}$ relative to the first.

$$b_y = -Bk_z\xi_y \quad (9)$$

To leading order, Ampère's law gives

$$j_z = \frac{1}{\mu_0}\frac{db_y}{dx} = -\frac{k_z BAe^{i\phi}}{\mu_0\delta_A^2\Delta} \cdot \frac{dF}{d\tau} \quad (10)$$

Thus j_z is determined by the variation of $F' = dF/d\tau$, which is displayed in Figure 3. The integral solution for F' is

$$F'(\tau) = \int_0^\infty iue^{-u^3/3}e^{iu\tau}du \quad (11)$$

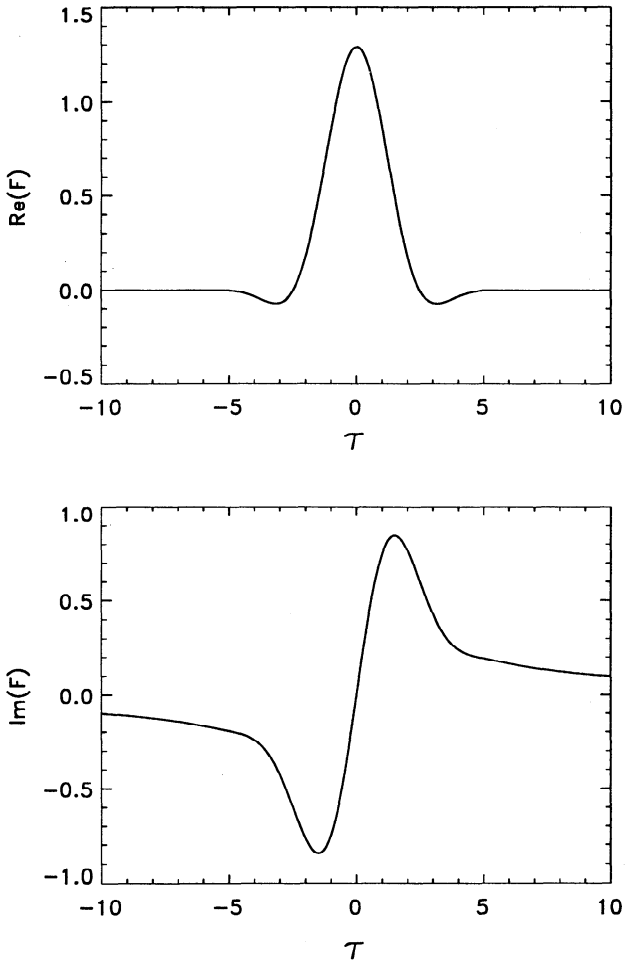

Figure 1. The universal function F for a resonance with nonzero η. (See also Figure 1 of GRH.) The top and bottom panels display the real and imaginary parts of F, respectively. The functions depend solely upon the normalized x coordinate τ.

To find the current that would be observed in a physical system, we need to include the explicit dependence of the mode on (y, z, t) and, for example, take the real part of the solution: $Re\{j_z(x)\sin(k_z z)\exp i(\phi + k_y y - \omega t)\}$

$$Re\{j_z(x,y,z,t)\} = -\frac{k_z BA}{2\mu_0 \delta_A^2 \Delta}\sin(k_z z)\left[F' e^{i\Phi} + F'^{*} e^{-i\Phi}\right] \tag{12}$$

where $\Phi = \phi + k_y y - \omega t$ and the asterisk denotes the complex conjugate. The dissipation rate is equal to $\mu_0\eta$ times the square of (12) and so has an x and t dependence of $[F'\exp(i\Phi) + F'^{*}\exp(-i\Phi)]^2$. Figure 4 shows the x (or τ) dependence as a function of time over one cycle of the heating perturbations. Note how the heating peaks move to larger τ as time increases. For the equilibrium considered by *Wright and Rickard* [1995], this maps to phase motion toward smaller x, consistent with the behavior derived numerically by them and shown in their Figure 12. The waves of ohmic heating propagating through the resonance region are directly analogous to effects observed in magnetospheric ultra-low-frequency (ULF) waves for the past three decades.

Contour plots of the ohmic heating versus t and τ are shown in Figure 5 (note that a maximum of heating occurs every half cycle of the wave). The resulting sloping contour patches are very reminiscent of the patches seen in auroral radar range-time-intensity (RTI) plots. Such slanting, repetitive patches were reported by *Kaneda et al.* [1964], *Keys* [1965], and *Brooks* [1967] and were interpreted as possibly being associated with hydromagnetic waves. A key feature of such events observed at middle to high magnetic latitudes was the apparent propagation through the radar backscatter region in a poleward direction. *Unwin and Knox* [1971] suggested that the electric field associated with a standing hydromagnetic wave was the source of the scattering region [see also *McDiarmid and McNamara,* 1973].

The reason for the apparent poleward propagation became clear after the field line resonance theory of magnetic pulsations [*Tamao,* 1965; *Southwood,* 1974; *Chen and Hasegawa,* 1974] was established. *Walker et al.* [1979] and *Greenwald and Walker* [1980] applied this theory to detailed observations of auroral pulsations observed using the Scandinavian Twin Auroral Radar Experiment. They showed that the apparent

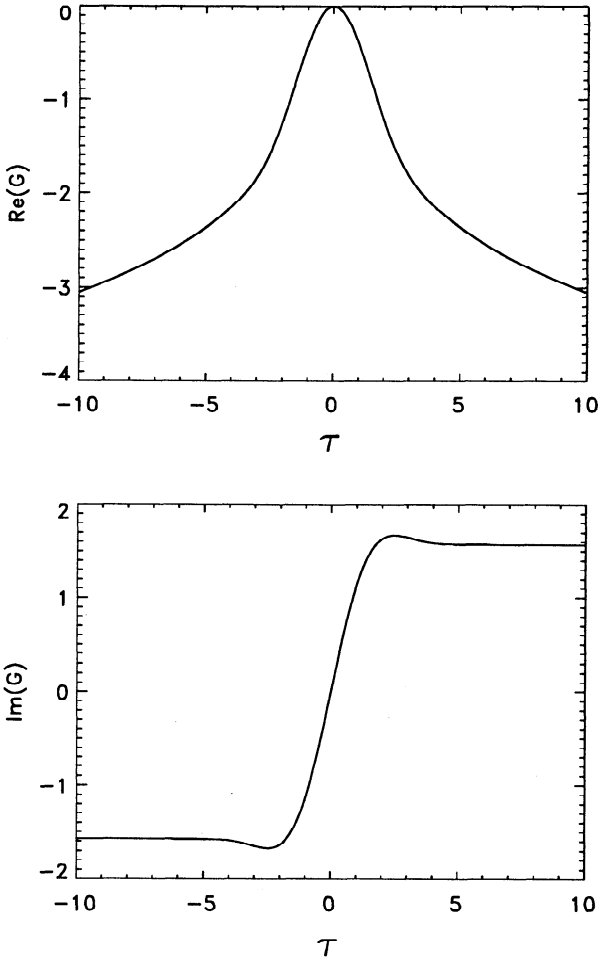

Figure 2. The universal function G for a resonance with nonzero η. (See also Figure 2 of GRH.) The top and bottom panels display the real and imaginary parts of G, respectively.

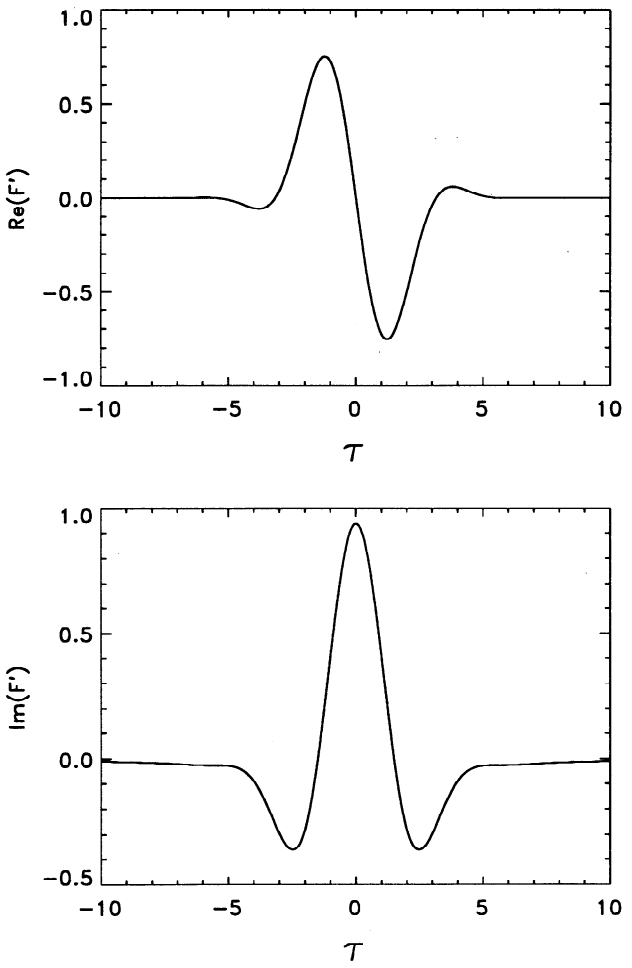

Figure 3. The derivative of the universal function F for a resonance with nonzero η. The top and bottom panels display the real and imaginary parts of $dF/d\tau$, respectively.

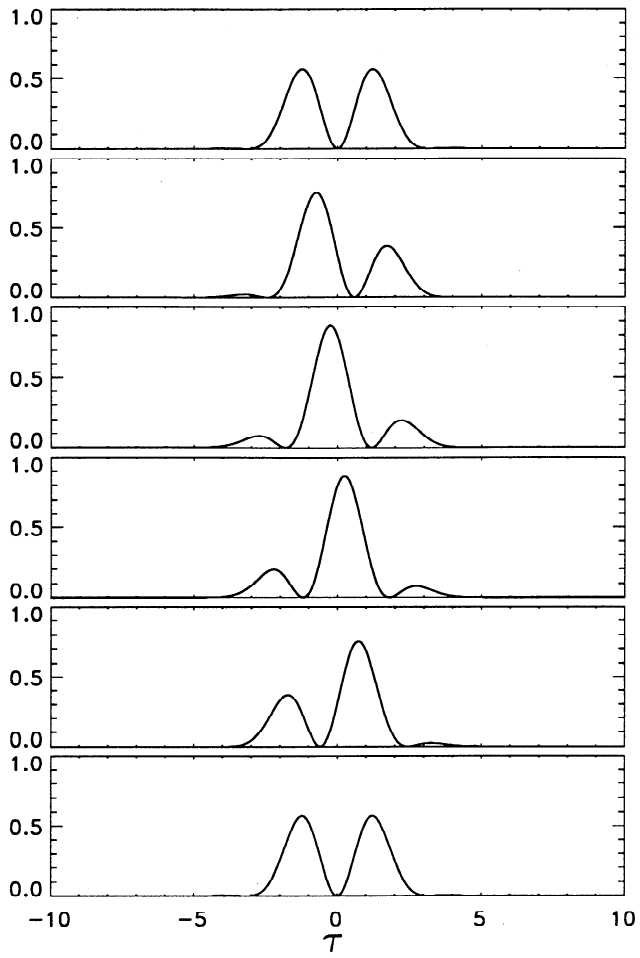

Figure 4. Snapshots of the spatial variation of ohmic heating for a resonance with nonzero η. The panels (from top to bottom) show the evolution through a half-period of the wave. Note how there is a phase motion of the peaks to larger τ.

poleward propagation was an artifact of the π phase change of the wave electric field through the resonance region. This leads to a zero of the electric field moving across the resonance region, giving a repetitive phase propagation [see *Knox and Allan,* 1980, Figure 3]. The phase propagation is always in the direction of decreasing Alfvén frequency ω_A, which is generally poleward in the outer magnetosphere. More discussion of the magnetospheric case will be given later. However, it is of interest to note that an effect which theory and simulation predict should occur in resonance structures in the solar atmosphere has a long history of experimental verification in the Earth's magnetosphere.

We now return to the observation of *Wright and Rickard* [1995] that the total heating rate over the volume is independent of time. Using the analytical solution of GRH, we find that the ohmic heating (OH) integrated over $-\infty < \tau < \infty$ and $-\ell < z < \ell$ is (see the appendix)

$$OH = \frac{\eta}{|\delta_A|^3 \Delta^2} \cdot \frac{\pi \ell k_z^2 B^2 A^2}{2\mu_0} \equiv \frac{1}{\omega |\Delta|} \cdot \frac{\pi \ell k_z^2 B^2 A^2}{2\mu_0} \quad (13)$$

There are several interesting features to note in this equation. The term involving η contains all the resistive dependence, and (4) was employed to get the final expression above. The familiar result of the total dis-

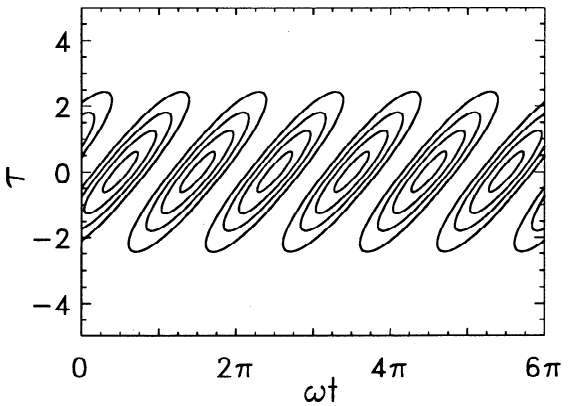

Figure 5. A contour plot of the ohmic heating rate as a function of t and τ for a resonance with nonzero η. The phase motion to larger τ is clear.

sipation being independent of η is now evident. The value of OH agrees with the time-averaged energy absorption rate from other models (see section 5). The proportionality of OH to $|d\omega_A^2/dx|^{-1}$ is also familiar [see, e.g., *Wright*, 1992, equation (18)]. The heating OH in (13) is, indeed, independent of time, and we have demonstrated *Wright and Rickard*'s [1995] assertion analytically. It is, perhaps, surprising that OH does not fluctuate over the wave cycle. There do not appear to be obvious physical grounds which require OH to be independent of time.

4. Resistive Boundary Solutions

In the magnetosphere the resistive dissipation in the body of the plasma is generally much less than in the ionospheric boundaries for ULF waves. We now address the structure of the Alfvén resonance in an ideal plasma whose background field threads a resistive ionospheric boundary. We set $\eta = 0$ in (3) and allow k_z to be complex [see *Southwood and Hughes*, 1983]

$$k_z = k_{zr} + ik_{zi} \tag{14}$$

If the boundaries are taken to be perfectly reflecting, for the moment, we find k_{zr} is determined by the quantization condition

$$k_{zr} = \frac{n\pi}{2\ell}, \qquad n = 1, 2, 3, \ldots \tag{15}$$

while k_{zi} is zero. If we now allow the boundaries to become slightly absorptive by introducing a finite height-integrated Pedersen conductivity (Σ_p), there is no first order change to the value of k_{zr} but k_{zi} now has magnitude

$$|k_{zi}| = \frac{k_{zr}}{\ell\omega\mu_0\Sigma_p} \tag{16}$$

The choice of time dependence in (1) means that we need to choose k_{zi} to be negative; this ensures that the Poynting flux is directed into the ionosphere which acts as a sink of energy.

The resistive boundary limits the singularity that would have occurred in the absence of dissipation. We can estimate the scale of the solution in the x direction by combining (3b) and (3d). In terms of the displacement we find an equation [e.g., *Southwood and Hughes*, 1983] which may be expanded about x_r to give

$$\left(\frac{\mu_0\rho(x_r)}{B^2}\omega^2 + \frac{\mu_0\rho'(x_r)}{B^2}\omega^2(x-x_r) + \ldots \right. \tag{17}$$
$$\left. -k_{zr}^2 - 2ik_{zr}k_{zi} + \ldots\right)\xi_y = ik_y\frac{b_z}{B}$$

Note from the definition of the Alfvén frequency that the first and third terms in brackets cancel exactly. The solution is affected by k_{zi} over a region where the two remaining bracketed terms in (17) are comparable. This defines a scale δ_B,

$$\delta_B\frac{\mu_0\rho'(x_r)\omega^2}{B^2} = 2k_{zr}k_{zi} \tag{18}$$

which may be rewritten

$$\delta_B = -2\frac{k_{zi}}{k_{zr}}\left(\frac{\omega^2}{d\omega_A^2/dx}\right)_{x_r} \tag{19}$$

Note that when Σ_p is very high, k_{zi} is very small. Thus we may employ δ_B as a small parameter with which to perturb the ideal set of equations [*Southwood and Hughes*, 1983]: Combining the governing equations (3) to give a single second-order equation for ξ_x close to the resonance region we find

$$\frac{d^2\xi_x}{dx^2} + \frac{1}{(x-x_r)-i\delta_B}\cdot\frac{d\xi_x}{dx} - k_y^2\xi_x = 0 \tag{20}$$

Changing to the dimensionless scaled variable

$$X = \frac{x-x_r}{\delta_B} \tag{21}$$

(20) becomes

$$\frac{d^2\xi_x}{dX^2} + \frac{1}{X-i}\cdot\frac{d\xi_x}{dX} = 0 + O(\delta_B^2) \tag{22}$$

the solution of which is

$$\xi_x = \xi_{x0}e^{i\phi}\mathcal{G}(X); \qquad \mathcal{G}(X) = \ln(X-i) \tag{23}$$

Leading order balance of (3e) gives $\xi_y = (i/k_y\delta_B)d\xi_x/dX$ or

$$\xi_y = -\xi_{x0}\frac{e^{i\phi}}{k_y\delta_B}\mathcal{F}(X); \qquad \mathcal{F}(X) = \frac{-i}{X-i} \tag{24}$$

The logarithmic and $1/X$ behavior are familiar results but are represented here as the universal functions $\mathcal{F}(X)$ and $\mathcal{G}(X)$, which are the counterparts of GRH's F and G functions. Figures 6 and 7 display the functions $\mathcal{F}(X)$ and $\mathcal{G}(X)$ which may be used to describe the velocity and magnetic fields across the resonant layer for an arbitrary Σ_p by transforming the solution back to real space (x). Note the similarities between our $\mathcal{F}(X)$ and $\mathcal{G}(X)$ and GRH's $F(\tau)$ and $G(\tau)$. The explicit expressions for the real and imaginary parts of $\mathcal{F}(X)$ and $\mathcal{G}(X)$ are quite straightforward,

$$\mathcal{F}_r(X) = (X^2+1)^{-1} \tag{25a}$$
$$\mathcal{F}_i(X) = -X(X^2+1)^{-1} \tag{25b}$$
$$\mathcal{G}_r(X) = \ln\sqrt{X^2+1} \tag{25c}$$
$$\mathcal{G}_i(X) = \tan^{-1}(-1/X) - \pi \quad X<0 \tag{25d}$$
$$\mathcal{G}_i(X) = \tan^{-1}(-1/X) \quad X>0 \tag{25e}$$

In the section 3 it was mentioned that poleward motion of the poloidal electric field (E_x) was commonly observed. We can confirm that this is also a feature of the solution presented here by constructing the real part of the complex function $(E_{x0}/k_y\delta_B)\cos(k_z z)\mathcal{F}(X)\exp i\Phi$, where $E_{x0} = \omega B\xi_{x0}$ and $\Phi = k_y y - \omega t + \phi - \pi/2$. Noting that $\cos(k_z z) \approx \cos(k_{zr}z) - ik_{zi}z\sin(k_{zr}z)$, we find

$$Re\{E_x(x,y,z=+\ell,t)\} \tag{26}$$
$$= E_{x0}\frac{k_{zi}\ell}{k_y\delta_B}[\cos(\Phi)\mathcal{F}_i(X) + \sin(\Phi)\mathcal{F}_r(X)]$$

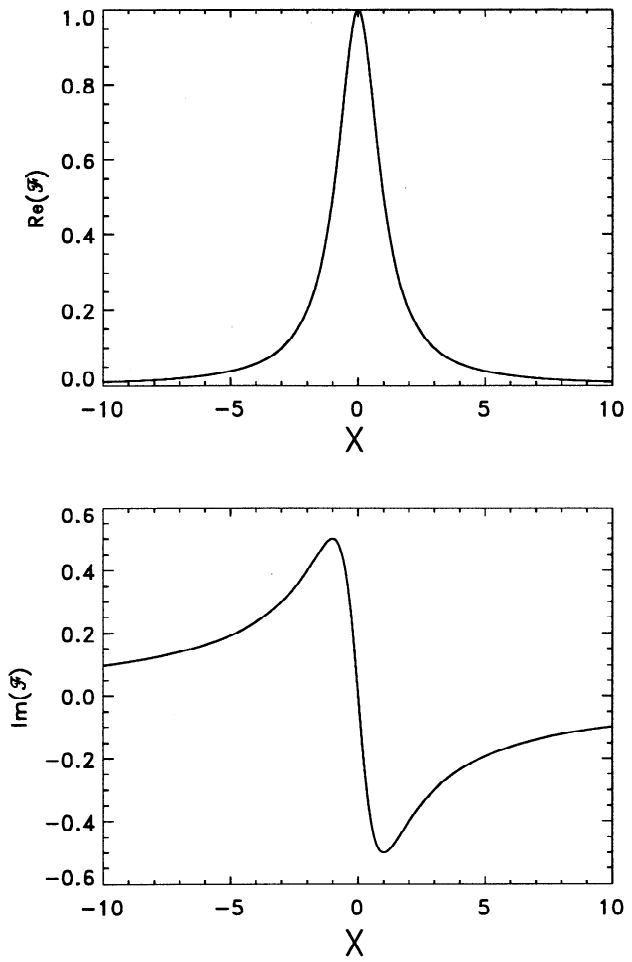

Figure 6. The universal function $\mathcal{F}$ for a resonance with finite Σ_p. The top and bottom panels display the real and imaginary parts of $\mathcal{F}$, respectively. The functions depend solely upon the normalized x coordinate X. (Note the similarity with Figure 1.)

Figure 8 shows the evolution of the electric field component E_x (actually the terms in square brackets in (26)) through the resonance region over one wave cycle in terms of the scaled variable X. The displacement ξ_y has a similar variation. The universal function $\mathcal{F}(X)$ generates a phase propagation in the direction of decreasing X. When mapped to the physical coordinate x (using (21)), the propagation is in the direction of decreasing ω_A. This behavior is consistent with the schematic in Figure 3 of *Knox and Allan* [1980].

Figure 9 shows a contour plot of E_x versus t and X over three wave cycles, with negative contours shown dashed. The slope of the contour patches in the resonance region again indicates phase propagation in the negative X direction, i.e. in the direction of decreasing ω_A. If a constant background electric field (of positive sign, say) were present in the ionosphere, the net negative electric field might drop below the threshold for backscatter, and only the positive patches (shown by full contours) would be seen by an auroral radar. It should be noted, however, that the structure of the universal function $\mathcal{F}(X)$ is independent of the ionospheric Pedersen conductance Σ_P, which enters through the scaling factor δ_B when converting to the physical coordinate x.

It is interesting to calculate the integrated energy dissipation per unit length in the $\hat{\mathbf{y}}$ direction within the resistive boundaries and see how this varies as a function of time. The dissipation rate per unit area at $z = +\ell$ is $\Sigma_p Re\{E_x\}^2$, and employing (26) this becomes

$$\Sigma_p E_{xr}^2 = \Sigma_p E_{xo}^2 \frac{k_{zi}^2 \ell^2}{k_y^2 \delta_B^2} \left[\mathcal{F}_i^2 \cos^2\Phi + \mathcal{F}_r^2 \sin^2\Phi + 2\mathcal{F}_r\mathcal{F}_i \sin\Phi\cos\Phi\right] \quad (27)$$

We need to integrate (27) over $-\infty < x < \infty$ to find OH, and note that $\int_{-\infty}^{+\infty} dx \equiv |\delta_B| \int_{-\infty}^{+\infty} dX$. On integration the term $\mathcal{F}_r\mathcal{F}_i$ yields zero as it is an odd function. Employing the following identities

$$\int_{-\infty}^{\infty} \mathcal{F}_r^2 dX \equiv \int_{-\infty}^{\infty} \mathcal{F}_i^2 dX \equiv \frac{1}{2}\int_{-\infty}^{\infty} |\mathcal{F}|^2 dX \equiv \frac{\pi}{2} \quad (28)$$

the integral of (27) gives the ohmic heating (OH) per unit y as

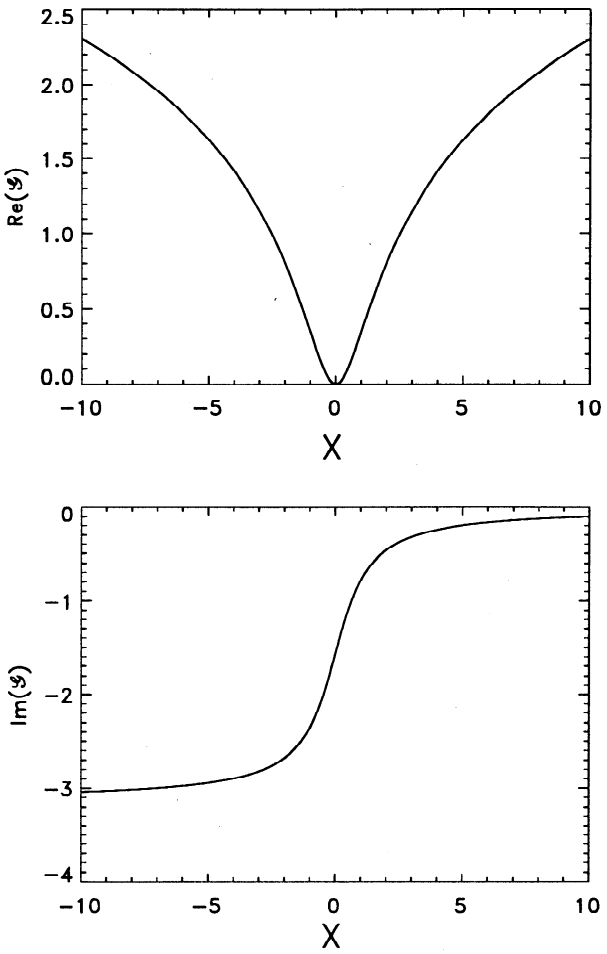

Figure 7. The universal function $\mathcal{G}$ for a resonance with finite Σ_p. The top and bottom panels display the real and imaginary parts of $\mathcal{G}$, respectively. The functions depend solely upon the normalized x coordinate X. (Note the similarity with Figure 2.)

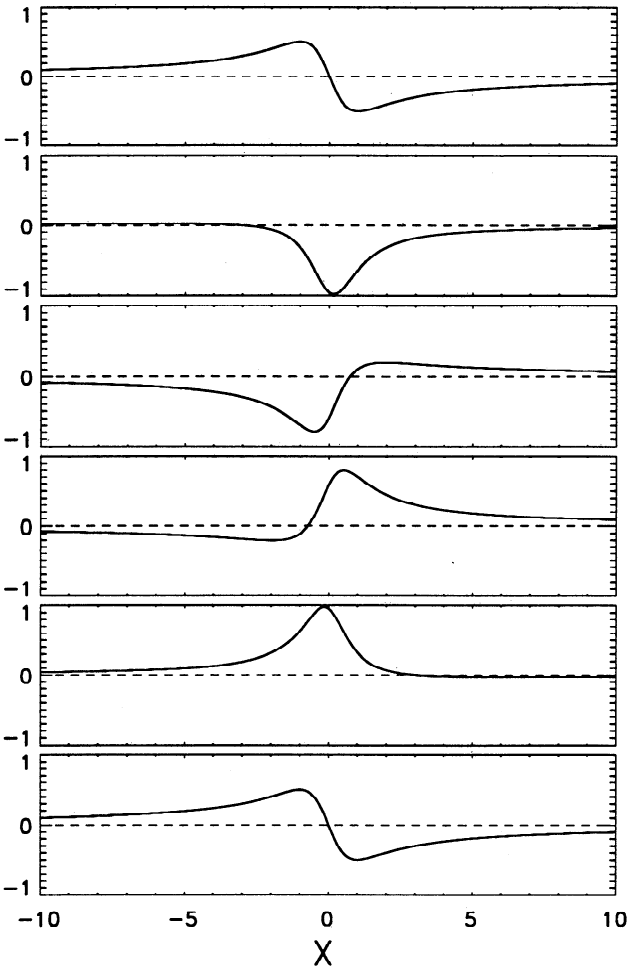

Figure 8. Snapshots of the spatial variation of E_x for a resonance with finite Σ_p. The panels (from top to bottom) show the evolution through one period of the wave. Note how there is a phase motion of the peaks and troughs to smaller X.

$$OH = \Sigma_p E_{xo}^2 \frac{k_{zi}^2 \ell^2}{k_y^2 |\delta_B|} \int_{-\infty}^{\infty} |\mathcal{F}|^2 \, dX = \Sigma_p E_{xo}^2 \frac{\pi k_{zi}^2 \ell^2}{k_y^2 |\delta_B|} \quad (29)$$

where a factor of 2 has been included to account for both ionospheres. Note that OH is once more independent of time. Moreover, recalling that k_{zi} and δ_B are both proportional to $1/\Sigma_p$, we see that OH is independent of Σ_p.

5. Discussion

In sections 3 and 4 we have derived analytical solutions for an Alfvén resonance whose singularity is resolved by some dissipation in the system. For both models we find that the rate of energy absorption by the resonance is independent of the dissipation coefficient, and we show later in this section that this is equal to the time-averaged jump in the Poynting flux across the singularity that occurs in the ideal set of MHD equations.

Although the two cases we consider have different dissipation mechanisms, we find that the universal functions from which the components of wave field and displacement are constructed are very similar. Note that although some of the $\mathcal{F}$ or $\mathcal{G}$ functions have opposite symmetry from their F and G counterparts, this merely produces oppositely directed phase motion in the scaled coordinates X and τ. What is important is the phase motion in real space (x), and for both models this is toward lower ω_A. Indeed, the forms of the perturbations are remarkably similar given the different dissipation mechanisms (dependent upon F' in the resistive plasma case but $\mathcal{F}$ in the resistive boundary case) and suggest that Alfvén resonances have a rather robust structure.

The two dissipative solutions we have derived have natural scale lengths of δ_A and δ_B over which the dissipation is important and determines the structure of the waves. Far away from the resonance ($|x| >> |\delta_A|$ or $|\delta_B|$) the exact nature of the dissipation does not affect the leading order behavior of the waves. Hence it is possible to compare the two values of OH derived in the paper (these should be identical if we set the two waves to have the same amplitude at large $|x|$).

We begin by relating the amplitudes of the two solutions A and E_{x0}. GRH give the asymptotic behavior of $F(\tau)$ as $\tau \to \infty$

$$F(\tau) \approx \frac{i}{\tau} \quad (30)$$

Thus the leading order behavior of (8) when $|x - x_r| >> |\delta_A|$ is

$$\xi_y \approx \frac{iAe^{i\phi}}{\Delta} \cdot \frac{1}{x - x_r} \quad (31)$$

The corresponding electric field is $E_x = i\omega \xi_y B$ and has the behavior

$$E_x = -\frac{\omega B A e^{i\phi}}{\Delta} \cdot \frac{1}{x - x_r} \quad (32)$$

The asymptotic behavior of E_x from the calculation in section 4 requires determining the asymptotic behavior

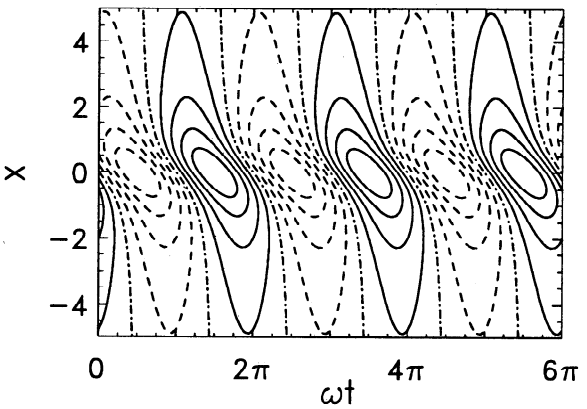

Figure 9. A contour plot of E_x as a function of t and X for a resonance with finite Σ_p. The phase motion to smaller X is clear. Figure 9 is similar to range-time-intensity plots familiar from observations [e.g., *Kaneda et al.*, 1964]. Full contours are positive, dashed contours are negative, and the dashed-dotted lines show zero contours.

of $\mathcal{F}(X)$. From (24) we find $\mathcal{F}(X) \approx -i/X$ when $|x - x_r| >> |\delta_B|$. Recalling that $E_x = -i(E_{x0}\exp(i\phi)/k_y\delta_B) \cdot \mathcal{F}(X)$, the asymptotic behavior of E_x for this model is

$$E_x = -\frac{E_{x0}e^{i\phi}}{k_y} \cdot \frac{1}{x - x_r} \tag{33}$$

Comparing (32) and (33), we see that setting

$$A = \frac{\Delta}{\omega B k_y} \cdot E_{x0} \tag{34}$$

will give the two solutions identical amplitudes far away from the resonance where the nature of the dissipation is unimportant. Employing (34), both expressions for OH (13) and (29) can be manipulated with straightforward algebra to yield the same result of

$$OH = E_{xo}^2 \frac{\pi}{2} \cdot \frac{\ell k_z^2}{\mu_0 k_y^2 \omega^3} \cdot \left|\frac{d\omega_A^2}{dx}\right|_{x_r} \tag{35}$$

so both models do indeed give identical dissipation rates. Note that since this dissipation rate is constant in time, it should be equal to the time-averaged jump in Poynting flux across the resonance that has been calculated in several ideal models. We now employ the results of one model that specifically considered the box model geometry. Equation (38) of *Thompson and Wright* [1993] states the time-averaged Poynting flux discontinuity as being

$$[\langle S_x \rangle] = \pi\omega^2 |\beta_0|^2 \langle \phi_r \rho \phi_r \rangle \left|\frac{d\omega_A}{dx}\right|_{x_r} \tag{36}$$

where $\phi_r(z)$ is the form of the Alfvén mode ($\sin(k_z z)$ or $\cos(k_z z)$ in our case) and the angle brackets denote integration along the length of the resonant field line. In our present model the density is independent of z and so may be taken outside of the brackets, which then integrate trivially to yield a value of ℓ. Writing $d\omega_A/dx = (d\omega_A^2/dx)/(2\omega_A)$ and noting that $\beta_0 \equiv i\exp(i\phi)A/\Delta$, the jump in Poynting flux may be expressed with the use of (34) as

$$[\langle S_x \rangle] = \frac{\pi}{2}\omega \left(\frac{E_{xo}^2}{\omega^2 B^2 k_y^2}\right) \rho(x_r)\ell \left|\frac{d\omega_A^2}{dx}\right|_{x_r} \tag{37}$$

Substituting $\rho(x_r)/B^2 \equiv k_z^2/(\omega^2\mu_0)$, we see that (37) is identical to (35). Thus the rate at which energy is supplied to the resonance from an ideal calculation is equal to the rate at which it is dissipated when η or Σ_p determine the structure of the resonance, as we would expect.

Note again that the spatially integrated dissipation within the resonance region is independent of time, while the energy input via the Poynting flux S_x is a time-dependent quantity proportional to $\cos^2(\omega t)$. This is quite a surprising result but does not violate continuity of energy, as one may suspect at first sight. The energy of the fields in the resonant layer (proportional to $|b_y|^2$ times the width) scales as $\eta^{-1/3}$ or Σ_p for the two cases we considered. Thus, in the limit of small dissipation the energy of the resonance becomes very large. The leading order $O(\eta^{-1/3}, \Sigma_p)$ of continuity of energy simply states that the energy within the resonance is constant in time. This is not surprising for Alfvén waves; they simply exchange energy back and forth between kinetic and magnetic energies. At the next order we have dissipation and influx of energy of the order of 1, i.e., $O(\eta^0, \Sigma_p^0)$. Note that the source and sink can not balance as the sink is independent of time, while the source varies as $\cos^2(\omega t)$. Continuity of energy at this order tells us that the energy stored in the resonant layer must change by the order of 1 during a cycle. This is a small change compared to the leading order energy $O(\eta^{-1/3}, \Sigma_p)$ and can be accommodated by introducing a correction of the order of 1 to the fields in the resonant layer, which have a leading order amplitude of $O(\eta^{-1/3}, \Sigma_p)$. Thus the leading order solution presented here is unaffected. The small correction could be calculated by retaining higher-order terms than the linear ones employed in the present analysis.

The solutions we have considered in sections 3 and 4 both contain some dissipation that allows transients to decay leaving the normal modes we derived as the asymptotic state. However, it is not necesary to have dissipation to achieve this result, and "leaky" boundaries will suffice as they appear to the system as a sink of energy. Indeed, *Berghmans and De Bruyne* [1995] addressed wave leakage through the photospheric boundaries of coronal loops by estimating the reflection coefficient (R) associated with the jump in density there. They set $k_y = 0$ in their calculation and so focused solely on Alfvén oscillations. However, many features of their resonance are similar to our dissipative boundary solution in section 4. For example, our dissipation is proportional to $1/\Sigma_p$, whereas in the work of *Berghmans and De Bruyne* [1995] the analogous quantity is $1 - R$. We find that the amplitude of the resonance scales as Σ_p (from (16), (19), and (24)), and the corresponding result of *Berghmans and De Bruyne* gives a scaling proportional to $1/(1 - R)$. In a similar fashion we would expect that the width of their resonance scales as $1 - R$, although this result was not explicity determined. It is interesting to note that the non-self-adjoint nature of dissipative MHD can be mimicked by having leaky (non-self-adjoint) boundary conditions on an ideal MHD plasma.

6. Summary

We have been concerned with normal mode solutions of the cold linearized MHD equations in a one-dimensional uniform box with uniform magnetic field, and density solely a function of x. Two cases have been considered, namely, (1) magnetic diffusivity η within the body of the plasma is significant, but the boundaries are perfect reflectors so that the parallel wavenumber k_z is real, and (2) η is negligible, but the boundaries have a finite Pedersen conductance Σ_P. As a consequence, k_z is complex and the boundaries absorb energy.

Case (1) relates to work by GRH and *Wright and Rickard* [1995] and is thought to be applicable to resonant wave coupling in solar coronal flux tubes. GRH showed that the Alfvén resonance region has a finite width due to the finite value of η and that the structure in the resistive layer around the resonance position can be described in terms of universal functions F and G, defined as integrals which are independent of η. *Wright and Rickard* [1995] investigated the structure of the resonance numerically, and showed that waves of ohmic heating propagate through the resistive layer. They also noted that the total heating rate over the volume is independent of time.

We have confirmed the numerical results of *Wright and Rickard* [1995] analytically by using the F and G functions to derive ohmic heating waves which propagate in the direction of decreasing Alfvén frequency and have shown that the volume-integrated heating rate is indeed independent of time (and of η). The heating waves are an artifact of the π phase change of the wave electric field through the resonance region, a feature which has been observed in magnetospheric Alfvén resonances for three decades.

Case (2) relates to Alfvén resonances in the magnetosphere. We have derived equivalent universal functions to those in case (1), which we denote by $\mathcal{F}$ and $\mathcal{G}$. These are independent of the ionospheric conductance Σ_P and have much simpler forms than F and G. However, their spatial properties are similar, leading to the same features as in case (1), namely, the propagation of ionospheric Joule heating waves in the direction of decreasing Alfvén frequency and the time independence of the ionospheric area-integrated heating rate. The latter is also independent of Σ_P.

The similarity of the universal functions in two cases with very different dissipation mechanisms suggests that Alfvén resonances have a robust basic structure. We have also shown that the two cases give identical total heating rates when the amplitudes are the same at large distances from the resonance position. The jump in Poynting flux across the resonance from an ideal calculation is shown to be equal to the rate at which energy is dissipated when η or Σ_p determine the structure of the resonance. However, it is a surprising result that the spatially integrated dissipation within the resonance region is independent of time when either η or Σ_p^{-1} are nonzero (mathematically this may be expressed as requiring $\int F'^2 dx$ or $\int \mathcal{F}^2 dx$ to vanish when integrated over $-\infty < x < \infty$). This property seems to be independent of the dissipation mechanism, and we do not understand why resonances should behave in this fashion. It will be interesting to see if solutions governed by different dissipation mechanisms, such as viscosity, display this property.

Appendix

In this appendix we prove that the total ohmic heating in a resistive Alfvén resonance is independent of time. For small η the heating is dominated by the j_z current. We need to calculate $\mu_0 \eta Re\{j_z\}^2$ by employing (12)

$$\mu_0 \eta Re\{j_z\}^2 = \frac{\eta k_z^2 B^2 A^2}{4\mu_0 \delta_A^4 \Delta^2} \sin^2(k_z z)\left[F'^2 e^{2i\Phi} + F'^{*2} e^{-2i\Phi} + 2F'F'^*\right] \quad (38)$$

We now integrate this relation over x and note that $\int_{-\infty}^{+\infty} dx = |\delta_A| \int_{-\infty}^{+\infty} d\tau$ to find that the first term in square brackets is proportional to

$$\int_{-\infty}^{\infty} F'^2 d\tau = \int_{-\infty}^{\infty} \left(F_r'^2 - F_i'^2 + 2iF_r'F_i'\right) d\tau \quad (39)$$

The final term in the integrand is an odd function of τ and so integrates to zero. The first term of the integral may be written (with the aid of (11))

$$\int_{-\infty}^{\infty} \left[\int_0^{\infty} -ue^{-u^3/3} \sin(u\tau) du\right]^2 d\tau \equiv \int_{-\infty}^{\infty} \left[\int_0^{\infty} ue^{-u^3/3} \cos(u\tau') du\right]^2 d\tau' \quad (40)$$

The equivalence follows from making the substitution $\tau = \tau' - \pi/2u$. It is evident from (11) that the integrand on the right-hand side of (40) is equal to $F_i'^2(\tau')$. Noting that $|F'|^2 = F_r'^2 + F_i'^2$, we arrive at the following identities

$$\int_{-\infty}^{\infty} F_r'^2 d\tau \equiv \int_{-\infty}^{\infty} F_i'^2 d\tau \equiv \frac{1}{2} \int_{-\infty}^{\infty} |F'|^2 d\tau \equiv \frac{\pi}{2} \quad (41)$$

with the final value being determined numerically. Note the analogy with (28).

Returning to (39), we see that the first and second terms in brackets will cancel, so that the whole expression (proportional to the first term in brackets in (38)) is equal to zero. Since the second term in (38) is equal to the conjugate of the first, this too will integrate to zero. The only remaining contribution when (38) is integrated arises from the term $F'F'^* \equiv |F'|^2$ which is positive definite, and its integral may be evaluated from (41). Further integration in z gives the total ohmic dissipation to be

$$OH = \frac{\eta}{|\delta_A|^3 \Delta^2} \cdot \frac{k_z^2 \ell B^2 A^2}{2\mu_0} \int_{-\infty}^{\infty} |F'|^2 d\tau \quad (42)$$

from which equation (13) follows directly.

Acknowledgments. This work was carried out while A.N.W. was supported by a UK PPARC Advanced Fellowship, with partial support from the New Zealand Foundation for Research, Science and Technology (FRST). W.A. acknowledges support from FRST under contract CO1309.

The Editor thanks Marcel Goossens and a second referee for their assistance in evaluating this paper.

References

Allan, W., and F. B. Knox, A dipole field model for axisymmetric Alfvén waves with finite ionosphere conductivities, , *27*, 79, 1979.

Berghmans, D., and P. De Bruyne, Coronal loop oscillations driven by footpoint motions: Analytical results for a model problem, *Astrophys. J., 453,* 495, 1995.

Brooks, D., Radio auroral echoes associated with sudden commencements and their possible use in measurement of magnetospheric ion densities, *J. Atmos. Terr. Phys., 29,* 589, 1967.

Chen, L., and A. Hasegawa, A theory of long-period magnetic pulsations, *J. Geophys. Res., 79,* 1024, 1974.

Goossens, M., and M. S. Ruderman, Conservation laws and connection formulae for resonant MHD waves, *Phys. Scr. T, 60,* 171, 1995.

Goossens, M., M. S. Ruderman, and J. V. Hollweg, Dissipative MHD solutions for resonant Alfvén waves in 1-dimensional magnetic flux tubes, *Sol. Phys., 157,* 75, 1995.

Greenwald, R. A., and A. D. M. Walker, Energetics of long period resonant hydromagnetic waves, *Geophys. Res. Lett., 7,* 745, 1980.

Hollweg, J. V., and G. Yang, Resonance absorption of compressible magnetohydrodynamic waves at thin "surfaces," *J. Geophys. Res., 93,* 5423, 1988.

Ionson, J. A., Resonant absorption of Alfvénic surface waves and the heating of solar coronal loops, *Astrophys. J., 226,* 650, 1978.

Kaneda, E., S. Kokubun, T. Oguti, and T. Nagata, Auroral radar echoes associated with Pc5, *Rep. Ionos. Space Res. Jpn., 18,* 165, 1964.

Keys, J. G., Pulsating auroral radar echoes and their possible hydromagnetic association, *J. Atmos. Terr. Phys., 27,* 385, 1965.

Knox, F. B., and W. Allan, Damping and coupling of long-period hydromagnetic waves by the ionosphere, *J. Geomag. Geoelectr., 32,* suppl. II, SII 129, 1980.

McDiarmid, D. R., and A. G. McNamara, Radio aurora, storm sudden commencements, and hydromagnetic waves, *Can. J. Phys., 51,* 1261, 1973.

Newton, R. S., D. J. Southwood, and W. J. Hughes, Damping of geomagnetic pulsations by the ionosphere, *Planet. Space Sci., 26,* 201, 1978.

Southwood, D. J., Some features of field line resonances in the magnetosphere, , *22,* 483, 1974.

Southwood, D. J., and W. J. Hughes, Theory of hydromagnetic waves in the magnetosphere, *Space Sci. Rev., 35,* 301, 1983.

Tamao, T., Transmission and coupling resonance of hydromagnetic disturbances in the non-uniform Earth's magnetosphere, *Sci. Rep. Tohoku Univ., Ser. 5, 17,* 43, 1965.

Thompson, M. J., and A. N. Wright, Resonant Alfvén wave excitation in two-dimensional systems: Singularities in partial differential equations, *J. Geophys. Res., 98,* 15,541, 1993.

Unwin, R. S., and F. B. Knox, Radio aurora and electric fields, *Radio Sci., 6,* 1061, 1971.

Vaclavik, J., and K. Appert, Theory of plasma heating by low frequency waves: Magnetic pumping and Alfvén resonance heating, *Nucl. Fusion, 31,* 1945, 1991.

Walker, A. D. M., R. A. Greenwald, W. F. Stuart, and C. A. Green, Stare auroral radar observations of Pc5 geomagnetic pulsations, *J. Geophys. Res., 84,* 3373, 1979.

Wright, A. N., Coupling of fast and Alfvén modes in realistic magnetospheric geometries, *J. Geophys. Res., 97,* 6249, 1992.

Wright, A. N., and G. J. Rickard, A numerical study of resonant absorption in a magnetohydrodynamic cavity driven by a broadband spectrum, *Astrophys. J., 444,* 458, 1995.

W. Allan, National Institute of Water and Atmospheric Research, PO Box 14-901, Kilbirnie, Wellington, New Zealand. (email: w.allan@niwa.cri.nz)

A. N. Wright, Mathematical Institute, University of St. Andrews, St Andrews, Fife KY16 9SS, Scotland. (email: andy@dcs.st-and.ac.uk)

(Received January 26, 1996; revised March 12, 1996; accepted April 4, 1996.)